Stem Cell Reports
Article

ISSCR

OPEN ACCESS

HIC1 Represses *Atoh1* Transcription and Hair Cell Differentiation in the Cochlea

Dunia Abdul-Aziz,[1,2] Nicolai Hathiramani,[2] Lauren Phung,[2] Vittoria Sykopetrites,[2,3] and Albert S.B. Edge[1,2,4,*]

[1]Department of Otolaryngology, Harvard Medical School, Boston, MA, USA
[2]Eaton Peabody Laboratory, Massachusetts Eye and Ear, Boston, MA, USA
[3]Università degli Studi di Milano, Milan, Italy
[4]Harvard Stem Cell Institute, Cambridge, MA, USA
*Correspondence: albert_edge@meei.harvard.edu
https://doi.org/10.1016/j.stemcr.2021.02.022

SUMMARY

Across species, expression of the basic helix-loop-helix transcription factor ATOH1 promotes differentiation of cochlear supporting cells to sensory hair cells required for hearing. In mammals, this process is limited to development, whereas nonmammalian vertebrates can also regenerate hair cells after injury. The mechanistic basis for this difference is not fully understood. Hypermethylated in cancer 1 (HIC1) is a transcriptional repressor known to inhibit *Atoh1* in the cerebellum. We therefore investigated its potential role in cochlear hair cell differentiation. We find that *Hic1* is expressed throughout the postnatal murine cochlear sensory epithelium. In cochlear organoids, *Hic1* knockdown induces *Atoh1* expression and promotes hair cell differentiation, while *Hic1* overexpression hinders differentiation. Wild-type HIC1, but not the DNA-binding mutant C521S, suppresses activity of the *Atoh1* autoregulatory enhancer and blocks its responsiveness to β-catenin activation. Our findings reveal the importance of HIC1 repression of *Atoh1* in the cochlea, which may be targeted to promote hair cell regeneration.

INTRODUCTION

Within the cochlea, sensory hair cells reside interdigitated with specialized supporting cells and mechanotransduce sound into electrical signal that they transmit to auditory neurons. In the mature mammalian cochlea, these sensory hair cells and supporting cells do not turn over, and as a consequence, damage induced by factors such as noise and aging results in irreversible hearing loss (Doetzlhofer et al., 2006; White et al., 2006). However, spontaneous regeneration occurs in non-mammalian cochlear sensory epithelia as well as the mammalian vestibular epithelia (Atkinson et al., 2015; Corwin and Cotanche, 1988; Ryals and Rubel, 1988; Warchol, 2011). Recent results have also demonstrated spontaneous regeneration of hair cells after damage in the newborn mammalian cochlea (Bramhall et al., 2014; Cox et al., 2014; Hu et al., 2016), where, upon damage and loss of Notch-mediated lateral inhibition, progenitor cells, which comprise a subset of supporting cells, express the basic helix-loop-helix transcription factor ATOH1 and differentiate into hair cells. These progenitor cells, which are marked by the stem cell marker LGR5, are Wnt responsive and re-enter the cell cycle to asymmetrically divide into supporting cell and hair cell lineages (Bramhall et al., 2014; Chai et al., 2012; Shi et al., 2013). But the regenerative potential of the newborn mammalian cochlea is lost in the first postnatal week, even when driven with exogenous stimuli (including *Atoh1* activation) (Kelly et al., 2012; Samarajeewa et al., 2018; Shi et al., 2013). The quiescence of the cochlear progenitor cells in the maturing cochlea suggests a broadly repressive regulatory network, such as a nonpermissive chromatin signature. These observations have prompted us to study signals that modulate the epigenetic status of cochlear genes in the first postnatal week.

Hypermethylated in cancer 1 (HIC1) is an evolutionarily conserved transcriptional repressor that has been previously shown to directly bind to and suppress the regulatory regions around the *Atoh1* gene during cerebellar development (Briggs et al., 2008). *Atoh1* is highly expressed in cerebellar granule progenitor cells (CGPs), and its expression drops during their differentiation, concurrent with the rise of *Hic1* expression (Ben-Arie et al., 2000; Briggs et al., 2008; Jensen et al., 2004; Lumpkin et al., 2003). Knockdown of *Hic1* contributes to the formation of medulloblastoma, a cerebellar tumor characterized by reactivation of *Atoh1* expression (Ayrault et al., 2010; Briggs et al., 2008; Flora et al., 2009; Grausam et al., 2017; Jensen et al., 2004). The human HIC1 is deleted in the contiguous gene disorder Miller-Dieker syndrome (Carter et al., 2000; Grimm et al., 1999), and *Hic1* knockout mice are embryonic lethal with defective craniofacial, gastrointestinal tract, and kidney development. *Hic1*-deficient intestinal epithelium derived from conditional Hic1-*loxP*/*loxP* crossed with Villin-Cre mice demonstrated increased number of secretory Paneth cells, which are driven by the transcription factors ATOH1 and SOX9, suggesting that *Hic1* deletion potentiates *Atoh1* expression and intestinal Paneth cell differentiation (Janeckova et al., 2015). HIC1 represses *Atoh1* by a mechanism involving recruitment of corepressor complexes, including C-terminal binding

protein (CtBP) (Deltour et al., 2002), nucleosome remodeling and deacetylase (NuRD) (Van Rechem et al., 2010), and polycomb repressive complex 2 (PRC2) (Boulay et al., 2012), which mediate chromatin changes resulting in repression. In addition, HIC1 negatively regulates Wnt signaling through direct protein-protein interactions via recruitment of T cell factor (TCF) and β-catenin to nuclear "HIC1 bodies" (Valenta et al., 2006), thereby preventing β-catenin activation of Wnt-responsive genes, which include *Atoh1* (Shi et al., 2010). The role of HIC1 in the regulation of *Atoh1* and hair cell differentiation in the inner ear has not been examined.

We hypothesized that HIC1 could contribute to *Atoh1* repression in the cochlea through transcriptional regulation and interaction with Wnt. Using qRT-PCR and *in situ* hybridization specific to *Hic1*, we show here that *Hic1* is expressed ubiquitously in the postnatal murine sensory epithelium, including hair cells and supporting cells. We use a murine cochlear organoid system comprising expanded postnatal LGR5$^+$ progenitor cells to study the effect of HIC1 transcriptional silencing on activation of the *Atoh1* autoregulatory enhancer, expression of hair cell genes, and hair cell differentiation. We show that short hairpin (sh)RNA-mediated *Hic1* knockdown in inner ear organoids activates the *Atoh1* enhancer, increases expression of hair cell genes, and potentiates hair cell development. Conversely, forced overexpression of HIC1 inhibits hair cell differentiation. Using a luciferase reporter system to study the mechanism of HIC1-mediated repression of *Atoh1*, we demonstrate that wild-type HIC1, but not the zinc-finger DNA-binding mutant C521S, is able to inhibit Atoh1 and Wnt reporter activation. Together, our findings suggest an important role for HIC1 in mediating *Atoh1* repression, at least in part through repression of TCF/β-catenin signaling, and that its targeted inhibition may potentiate hair cell regeneration in the mature mammalian cochlea.

RESULTS

Hic1 is Expressed in the Sensory Epithelium of Postnatal Mice Across Developmental Time Points

Given the potential regulatory function of HIC1 in the mammalian cochlear sensory epithelium, we first probed its expression in newborn versus adult murine cochleae (Figure 1). qRT-PCR of dissected cochlear sensory epithelia from postnatal day 1 (P1), P7, and P14 mice demonstrated progressively increased expression of *Hic1*, while corresponding expression of *Atoh1* precipitously declined (Figure 1A). Immunohistochemistry using a commercially available HIC1 antibody showed nonspecific binding, as others have reported (Pospichalova et al., 2011). Therefore, to specify at the cellular level the relative expression of *Hic1* in the sensory epithelium (schematized in Figure 1B), we used single-molecule *in situ* hybridization to provide a semiquantitative and highly specific *Hic1* expression pattern in the cochlea (Figures 1C and S1) and control murine intestinal epithelia (Figure S1). Across ages, *Hic1* is expressed throughout the sensory epithelium, including hair cells, supporting cells, and cells of the medial and lateral compartments.

Hic1 Knockdown in Cochlear Organoids Activates the *Atoh1* Enhancer and Potentiates Hair Cell Differentiation

To investigate whether HIC1 activity is relevant to cochlear hair cell differentiation, we tested the effect of *Hic1* silencing on *Atoh1* expression and hair cell differentiation in cochlear organoids (Lenz et al., 2019; McLean et al., 2017). Inner ear organoids, similar to other tissue-specific organoid models (for example, the intestine, skin, or brain), recapitulate *in vivo* hair cell development (Clevers, 2016; Roccio and Edge, 2019). They are derived from newborn mouse cochlear sensory epithelia following an established protocol in which isolated LGR5$^+$ progenitor/supporting cells are selectively expanded and then induced to differentiate to immature hair cells that contain stereocilia and express key hair cell markers, including *Atoh1*, *Gfi1*, *Pou4f3*, and *Myo7a* (schematized in Figure 2A) (Lenz et al., 2019; McLean et al., 2017).

We examined the relationship between *Hic1* and *Atoh1* expression levels following shRNA-mediated knockdown of *Hic1*. In these experiments, we generated cochlear organoids from *Atoh1-nGFP* transgenic mice, which provide a reliable fluorescent reporter of *Atoh1* expression and hair cell differentiation by expression of GFP in hair cells under the control of the *Atoh1* 3′ enhancer (Abdolazimi et al., 2016; Lenz et al., 2019; Lumpkin et al., 2003; McLean et al., 2017). Organoids were analyzed at various time points of differentiation (D10, D15, D20), which reflect relative maturation of the hair cells (McLean et al., 2017). Dissociated cochlear progenitor cells were transduced with lentivirus delivering the pLKO-mScarlet vector, which results in constitutive expression of shRNA targeting *Hic1* (shHic1) or control nontargeting shRNA (shControl) and mScarlet to mark transduced cells. Following the initial 10 day proliferation period, live cell imaging and flow cytometry showed a significantly greater percentage of mScarlet$^+$/Atoh1-nGFP$^+$ double-positive cells in shHic1-infected cells as opposed to shControl (Figures 2B and 2C), indicating that *Hic1* knockdown alone (in the absence of any other differentiation-promoting factors) potentiates *Atoh1* expression. The proportion of Atoh1-nGFP$^+$ cells, indicative of *Atoh1* enhancer activation, in both transduced and untransduced cells was

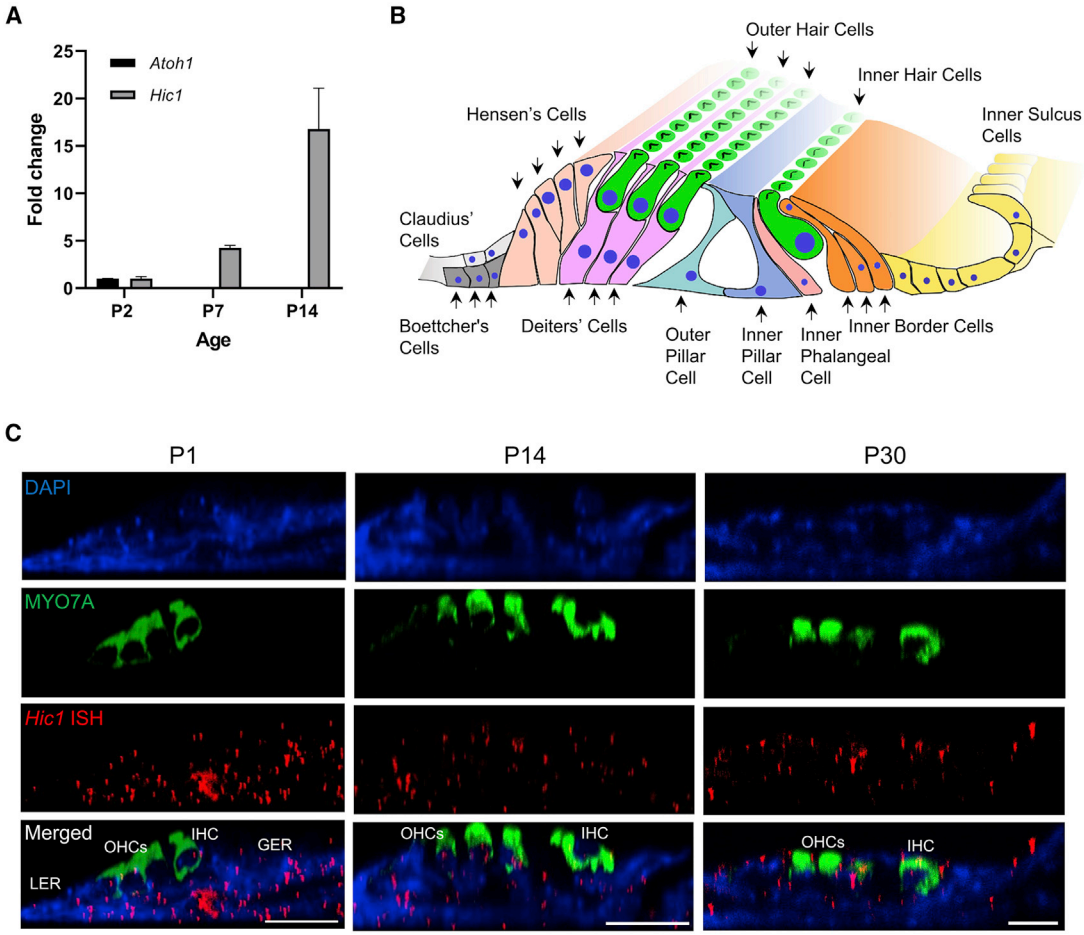

Figure 1. *Hic1* is Expressed in Postnatal Murine Sensory Epithelia Across Developmental Time Points Corresponding to Onset of Hearing

(A) mRNA levels of *Hic1* and *Atoh1* in dissected cochlear sensory epithelia (n $\geq$ 6 cochleae) at P2, P7, and P14 measured by qRT-PCR and normalized to *18S* show increased *Hic1* expression with age, while *Atoh1* level declines. Results are presented as fold change in expression normalized to P2.

(B) Schematic shows arrangement of sensory epithelial cells in the adult organ of Corti with supporting cells interdigitated among rows of outer and inner hair cells.

(C) Semiquantitative single-molecule *in situ* hybridization for *Hic1* (RNAscope) followed by MYO7A immunohistochemistry of fixed cochlea at P1, P14, and P30 demonstrating expression of *Hic1* throughout the cells comprising the cochlear sensory epithelium (see also Figure S1). Scale bar, 20 μm. GER, greater epithelial ridge; IHC, inner hair cell; LER, lesser epithelial ridge; OHC, outer hair cell.

highest at D10 and reflects the relative priming of progenitor cells that have an accessible/active *Atoh1* enhancer during the end of proliferation/start of differentiation period in organoids. This observation is consistent with single-cell expression data that demonstrate *Atoh1* expression levels to be highest at this early time point (Lenz et al., 2019). The ability of shHic1 alone to activate the Atoh1-nGFP reporter persisted over the 10 day window of differentiation studied, in marked contrast to untransduced and shControl-transduced cells in which Atoh1-nGFP activity decreased over time (D15; Figure 2C). These findings indicate that downregulation of HIC1 in supporting cells promotes *Atoh1* expression which is essential for differentiation to hair cells.

To confirm induction of hair cell fate, we performed immunostaining for an additional hair-cell-specific marker, Myosin VIIA (MYO7A), an unconventional myosin isozyme essential for hair cell function. Organoids were fixed and analyzed by high-resolution immunohistochemistry and showed significantly increased co-expression of mScarlet and MYO7A in a greater proportion of shHic1-treated organoids in contrast to shControl (Figure 2D). qRT-PCR analysis of sorted, transduced cells at 10 days of differentiation revealed significantly increased

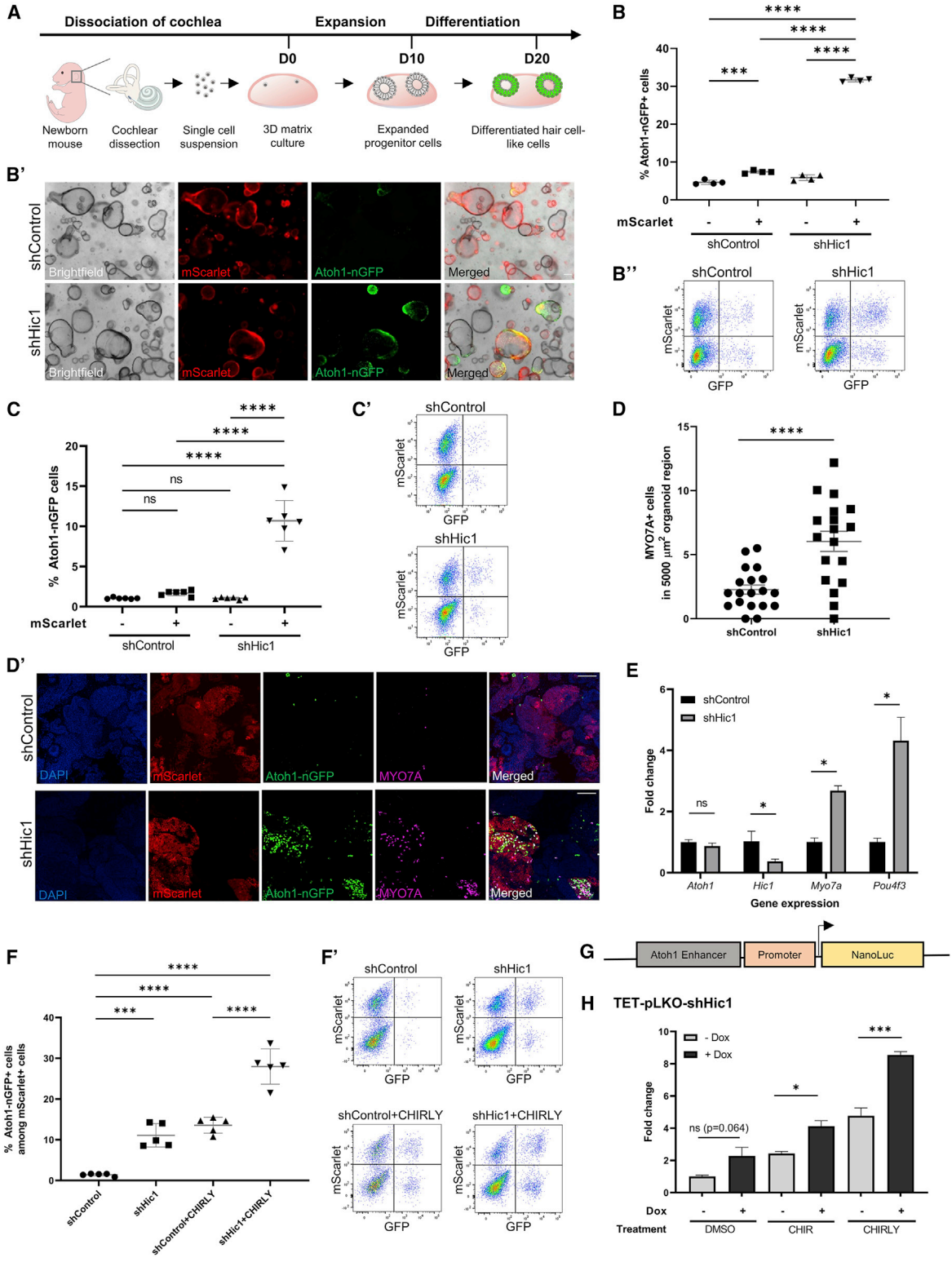

Figure 2. *Hic1* Knockdown in Cochlear Organoids Potentiates *Atoh1* Activation and Hair Cell Differentiation

(A) Schematic of the cochlear organoid protocol. Dissociated postnatal day 3 supporting cells isolated from wild-type or *Atoh1-nGFP* transgenic reporter mice are transduced at D0 with lentivirus and expanded in proliferation medium for 10 days, followed by induction of

(legend continued on next page)

levels of hair-cell-specific genes, *Myo7a* and *Pou4f3*, in shHic1-transduced cells (Figure 2E), which turn on after *Atoh1* induction during development (Cai and Groves, 2015).

Reminiscent of *in vivo* mammalian hair cell differentiation, expanded supporting cells in organoids do not spontaneously differentiate to *Atoh1*$^+$ hair cells to a significant degree (1%–5%) but can be potentiated through known pathways, including Wnt activation (McLean et al., 2017; Samarajeewa et al., 2018; Shi et al., 2010, 2013) and Notch inhibition (Abdolazimi et al., 2016; Brown and Groves, 2020; Jeon et al., 2011; Mizutari et al., 2013). Both Wnt and Notch pathways act through effector transcription factors, TCF/LEF and HES/HEY, respectively, at the *Atoh1* regulatory promoter and enhancer regions to regulate *Atoh1* at the transcriptional level. To assess the interplay of *Hic1* knockdown with these pathways and their potential to promote hair cell differentiation, organoids were treated with drugs that promote differentiation, the GSK3β inhibitor CHIR99021 (CHIR), to potentiate Wnt signaling, in combination with the Notch inhibitor LY411575 (LY), compared with vehicle control (DMSO), and analyzed by flow cytometry. Consistent with results from earlier time points, Atoh1-nGFP organoids transduced with shHic1 generated a significantly greater proportion of double-positive (GFP$^+$/mScarlet$^+$) cells and potentiated the effect of CHIR in combination with LY (CHIRLY) relative to shControl (Figure 2F).

In addition to the downstream 3′ enhancer, the *Atoh1* proximal promoter has been shown to be important in the regulation of *Atoh1* expression, being the primary site of action of HES/HEY repression by binding to canonical E-box C-site motifs (Figure S2) (Abdolazimi et al., 2016). Query of the murine *Atoh1* genomic locus for a biochemically determined HIC1 binding motif (TGCC[A/C]) (Pinte et al., 2004) reveals several putative binding sites (Figure S2), and publicly available chromatin immunoprecipitation sequencing (ChIP-seq) data of HIC1 binding in HEK293 cells provided through the ENCODE Project (dataset: ENCSR803GYT, www.encodeproject.org) (ENCODE

differentiation at D10. Analysis by immunofluorescence, RT-PCR, and flow cytometry was performed at various time points—D10, D15, and D20—of differentiation that correlate with relative maturation of hair cells in the organoids.

(B) Frequency of *Atoh1* activation (Atoh1-nGFP$^+$) in cochlear organoids among cells transduced (mScarlet$^+$) with shControl and shHic1 after initial 10 days of expansion (D10) as measured by flow cytometry (n = 4). At the onset of differentiation, when *Atoh1* levels are highest, significantly more supporting cells transduced with shHic1 activate the Atoh1-nGFP reporter relative to shControl (7.4% [±0.4] [shControl] versus 31.7% [±0.5] [shHic1]), as well as relative to untransduced mScarlet$^-$ populations in either group (4.7% [±0.6] [untransduced, shControl], 5.9% [±0.7] [untransduced, shHic1]).

(B′) Representative bright-field images showing greater proportion of double-positive (GFP$^+$/mScarlet$^+$) cells in shHic1-treated organoids relative to shControl. Scale bar, 150 μm.

(B″) Representative flow cytometry.

(C) Frequency of double-positive (GFP$^+$/mScarlet$^+$) cells among shHic1 and shControl transduced cells in D15 organoids as measured by flow cytometry, with representative plots (n = 5). With shControl, 1.7% (±0.3) of the total transduced mScarlet$^+$ supporting cells demonstrate persistent Atoh1-nGFP expression, while with shHic1, 10.7% (±2.5) of the total mScarlet$^+$ supporting cells activate Atoh1-nGFP.

(C′) Representative flow cytometry.

(D) Quantification (n $\geq$ 18 organoids) of the hair-cell-specific marker, MYO7A$^+$, in shControl and shHic1 organoids. Representative immunohistochemistry for mScarlet, Atoh1-nGFP, and MYO7A in cochlear organoids.

(D′) Hair cell differentiation and expression of hair-cell-specific markers, Atoh1-nGFP and MYO7A, are induced in a subset of organoids transduced with shHic1 (D15 organoids). Scale bar, 20 μm.

(E) mRNA expression of hair cell genes in D20 FACS-sorted, mScarlet$^+$ cells from shHic1 and shControl organoids. Knockdown of *Hic1* potentiates expression of hair cell transcripts, *Myo7a* and *Pou4f3*, following 10 days of differentiation. Results are presented as fold change in expression normalized to *Gapdh* relative to shControl. Student's t test, *p < 0.05.

(F) Frequency of *Atoh1* activation (Atoh1-nGFP$^+$) in cochlear organoids among cells transduced (mScarlet$^+$) with shControl and shHic1 alone and in combination with CHIRLY demonstrates that shHic1 augments CHIRLY to drive differentiation of supporting cells to hair cells, as measured by increased double-positive (GFP$^+$/mScarlet$^+$) cells in shHic1-treated cells, relative to shControl (D20 organoids, n = 5): shControl, 1.4% (±0.3); shHic1, 11.1% (±2.9); shControl + CHIRLY, 13.6% (±2.0); shHic1 + CHIRLY, 28.0% (±4.3).

(F′) Representative flow cytometry of different treatments.

(G) Schematic of the *Atoh1* enhancer-promoter-nanoLuc (Atoh1-Enh-Prom-NLuc) lentivirus construct.

(H) Results of dual nanoLuc/firefly luciferase reporter assay in cochlear organoids. Cochlear progenitor cells were transduced with Atoh1-Enh-Prom-NLuc reporter, constitutively active firefly luciferase control reporter, and TET-pLKO-shHic1 and subsequently differentiated with specified treatments with and without Dox (1 μg/mL), and the nanoLuc/firefly luciferase ratio was quantified. Knockdown of *Hic1* potentiates differentiation and activation of the *Atoh1* promoter and enhancer (n = 3): DMSO, 1.00 ± 0.09; DMSO + Dox, 2.28 ± 0.53; CHIR 2.44 ± 0.12; CHIR + Dox, 4.12 ± 0.34; CHIRLY, 4.78 ± 0.48; CHIRLY + Dox, 8.55 ± 0.20 (unless otherwise indicated, data reflect mean ± SD from n independent experiments; one-way ANOVA, *p < 0.05, ***p < 0.001, ****p < 0.0001).

Project Consortium, 2012; Davis et al., 2018) and visualized using the UCSC browser (genome.ucsc.edu) shows binding across the *ATOH1* locus, with a strong peak at the *ATOH1* proximal promoter (Figure S3). By comparison with the *ATOH1* promoter, the minimal β-globin promoter used in Atoh1-nGFP transgenic mice and in the *Atoh1* enhancer luciferase reporter lacks putative HIC1 binding sites and demonstrates no significant signal in HIC1 ChIP-seq. To investigate the combined contribution of the promoter and enhancer regions in *Atoh1* regulation, we developed a nanoLuc-based reporter system that incorporates the upstream promoter and 3′ enhancer regions of *Atoh1* (referred to as "Atoh1-Enh-Prom-NLuc") and tested the effect of *Hic1* silencing on reporter activity in inner ear organoids (Figure 2G). This assay provides a bulk assessment of reporter activation, as measured by a luminometer, in unsorted transduced organoids subject to different treatments that is distinct from and complementary to fluorescence-activated cell sorting (FACS)-based assays described earlier that quantify the effect of shHic1 knockdown at the individual cell level. It allows for the study of reporter function within the milieu of the differentiating organoids without reliance on transgenic mice or flow cytometry, but has the limitation of population-level readout. Inner ear organoids were transduced with lentiviruses carrying Atoh1-Enh-Prom-NLuc, firefly luciferase control, and doxycycline (Dox)-inducible shRNA targeting *Hic1* (TET-pLKO-mScarlet-shHic1). Expanded cochlear progenitor cells were induced to differentiate using drug treatments that promote differentiation, CHIR alone and CHIRLY, compared with control (DMSO). At the D10 differentiation time point, we varied the degree of *Hic1* knockdown by inclusion or absence of Dox (Figure 2H). The NanoLuc luciferase signal, normalized to baseline firefly luciferase level to control for cell density and transduction efficiency, was read out after 10 days of differentiation (Figure 2H). Consistent with the Atoh1-nGFP reporter mice, Dox-induced shRNA targeted to *Hic1* potentiated the activation of the Atoh1-Enh-Prom-NLuc reporter when combined with CHIR and CHIRLY, indicating a positive effect of *Hic1* knockdown on the average *Atoh1* expression within the organoids. Of note, the DMSO treatment group, which reflects the effect of shHic1 induction alone at D20 on Atoh1-Enh-Prom-NLuc activity, showed a trend consistent with FACS-based results, yet did not achieve statistical significance ($p = 0.064$), which likely reflects the limitations of the luciferase-based assay, which quantifies bulk expression changes in unsorted organoid populations. Overall, these findings suggest that *Hic1* knockdown in inner ear cells augmented the transcriptional stimulation induced by Wnt activation and by Notch inhibition, and that the repressive effect of HIC1 occurs at physiologic levels of the protein in the inner ear.

HIC1 Overexpression Suppresses *Atoh1* Activation and Hair Cell Differentiation in Cochlear Organoids

To further test the hypothesis that HIC1 represses *Atoh1* in the inner ear, we forced expression of HIC1 in organoids derived from Atoh1-nGFP mice using lentiviral delivery of *HIC1* under a Dox-inducible system, with mScarlet to mark transduced cells. Dissociated cochlear cells were transduced with Dox-inducible *HIC1* and, after 10 days of proliferation, organoids were forced to differentiate with CHIRLY, with (+) or without (−) Dox (Figure 3A). Relative to no-Dox control, mScarlet$^+$ cells in which HIC1 was overexpressed (+Dox) showed a 50% reduction in differentiation and Atoh1-nGFP co-expression, indicating that HIC1 suppresses *Atoh1* activation in these cells (Figures 3A and 3B). This suppression of GFP was not observed in transduced cells in which HIC1 overexpression was not induced (mScarlet$^+$, −Dox), or in untransduced cells treated with Dox (mScarlet$^-$, +Dox). There was no increased cell death with HIC1 overexpression, as assessed by live microscopy and DAPI viability gating across treatments. Together with the knockdown data, these findings indicate that HIC1 is a biologically relevant repressor of progenitor-to-hair cell differentiation in the ear.

HIC1 Represses the *Atoh1* Regulatory Enhancer

Hair cell differentiation is driven by the transcription factor ATOH1 through regulation of its 1.7 kb downstream enhancer as well as promoter regions (Figure 4; Figure S2) (Gálvez et al., 2017; Helms et al., 2000). Having observed that HIC1 knockdown and overexpression respectively increase and decrease hair cell differentiation in cochlear organoids, we proceeded to investigate whether HIC1 may act as a direct transcriptional regulator of *Atoh1*, as suggested by prior studies in the cerebellum where HIC1 was shown to directly bind to the two adjacent motifs in the *Atoh1* enhancer (Figure S2) (Briggs et al., 2008; Pinte et al., 2004). We therefore tested the effect of HIC1 on the *Atoh1* 3′ enhancer in an orthologous system, HEK293 cells, which do not naturally express *ATOH1* but do express *HIC1* (Broad Institute Cancer Cell Line Encyclopedia: portals.broadinstitute.org/ccle). Co-transfection of a reporter containing the *Atoh1* 3′ enhancer driving firefly luciferase with either a vector for constitutive HIC1 expression or a small interfering RNA (siRNA) targeting endogenous *HIC1* showed the same pattern as observed in organoids, an inverse relation between HIC1 expression and *Atoh1* enhancer activity, while empty vector or non-targeting siRNA had no effect (Figure 4A). ATOH1 is a potent activator of its own expression via its 3′ enhancer (Klisch et al., 2011), and our results in cochlear organoids leave open the possibility that the effect of HIC1 may be indirect through ATOH1 (for example, regulating an upstream factor, which then turns on *Atoh1* expression). Given the

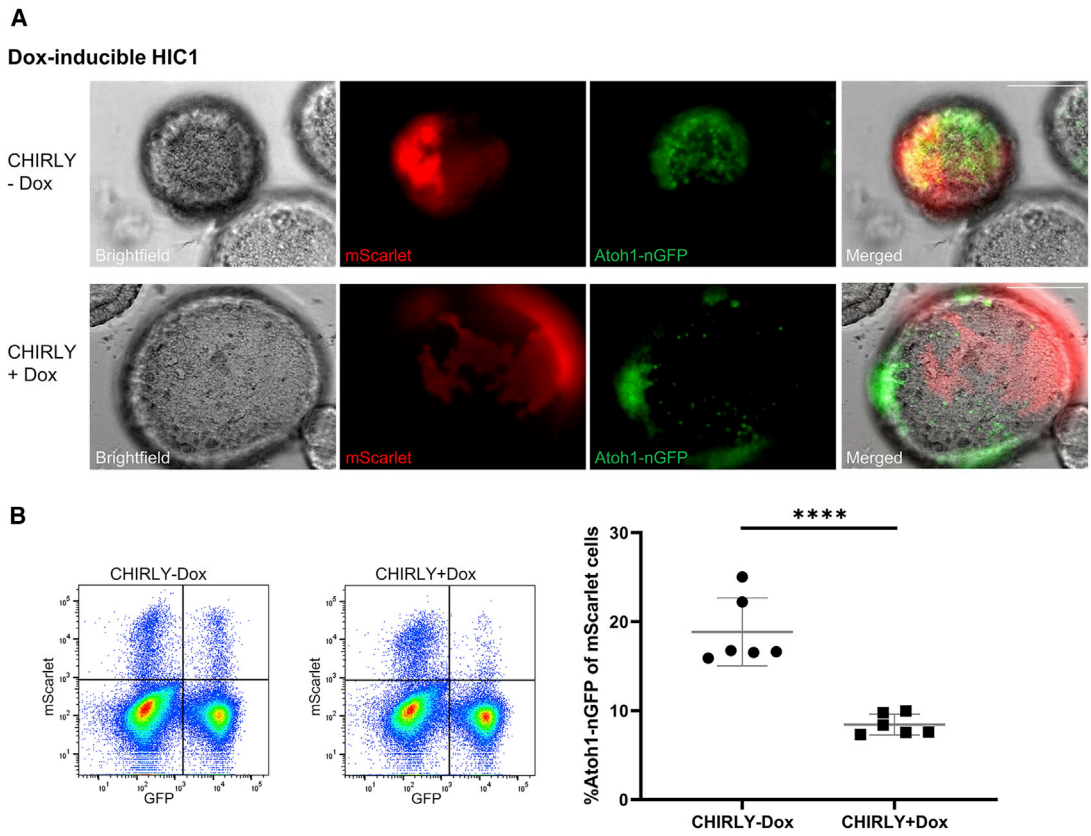

Figure 3. HIC1 Overexpression Inhibits Hair Cell Differentiation

(A) Representative bright-field microscopy of D20 organoids (mScarlet$^+$) transduced with doxycycline-inducible *HIC1* and differentiated with CHIRLY demonstrates loss of Atoh1-nGFP activation in mScarlet$^+$ cells in which HIC1 overexpression was induced (+Dox). Scale bar, 150 μm.

(B) Frequency of Atoh1-nGFP$^+$/mScarlet$^+$ cells among cells transduced with doxycycline-inducible *HIC1* (mScarlet$^+$) cells in CHIRLY-treated cochlear organoids (D20 organoids). HIC1 overexpression (+Dox) significantly inhibits (approximately 50%) CHIRLY-driven differentiation and Atoh1-nGFP reporter expression relative to control (n = 6). Data reflect mean ± SD; Student's t test, ****p < 0.0001.

absence of ATOH1 in HEK cells, these data indicate that HIC1 regulates *Atoh1* by interacting with the 3′ enhancer and is independent of the ATOH1 protein.

HIC1 Inhibits TCF/β-Catenin Activation of *Atoh1*

The activation of *Atoh1* by Wnt and subsequent loss of *Atoh1* responsiveness to Wnt are critical events regulating hair cell development (Samarajeewa et al., 2018; Shi et al., 2010). We therefore investigated whether HIC1 represses *Atoh1* by inhibiting its activation by Wnt. Indeed, co-transfection of HEK293 cells with the *Atoh1* enhancer reporter and β-catenin show activation of *Atoh1* expression, as expected, and this activation is increased by knockdown of endogenous HIC1 and reversed by addition of exogenous HIC1 (Figure 4B) in a dose-dependent fashion (Figure 4C).

The *Atoh1* gene locus contains several sites matching the HIC1 minimal DNA binding motif TGCC(A/C) (Figure S2), and ChIP-qPCR data indicate HIC1 occupancy at some of these sites (Briggs et al., 2008; Pinte et al., 2004). To test whether DNA binding is required for HIC1 regulation of *Atoh1*, we employed a previously characterized mutant of HIC1, which contains an amino acid substitution (C521S) in the third zinc-finger domain that abolishes DNA binding and repression activity (Figure 4B) (Pinte et al., 2004). We confirmed that wild-type HIC1 and not HIC1 C521S represses the HIC1 reporter (5×HiRE), as shown previously (Figure 4D) (Pinte et al., 2004). We found that HIC1 C521S is less effective at blocking *Atoh1* enhancer activation by β-catenin (Figure 4A), supporting the view that HIC1 regulation of *Atoh1* requires direct binding to the enhancer.

However, prior work has shown that HIC1 can inhibit β-catenin at the protein level by sequestering β-catenin/TCF in a nuclear complex with HIC1 (Valenta et al., 2006). Using an established TCF reporter, pTOPflash, which comprises evenly spaced repeat TCF binding motifs,

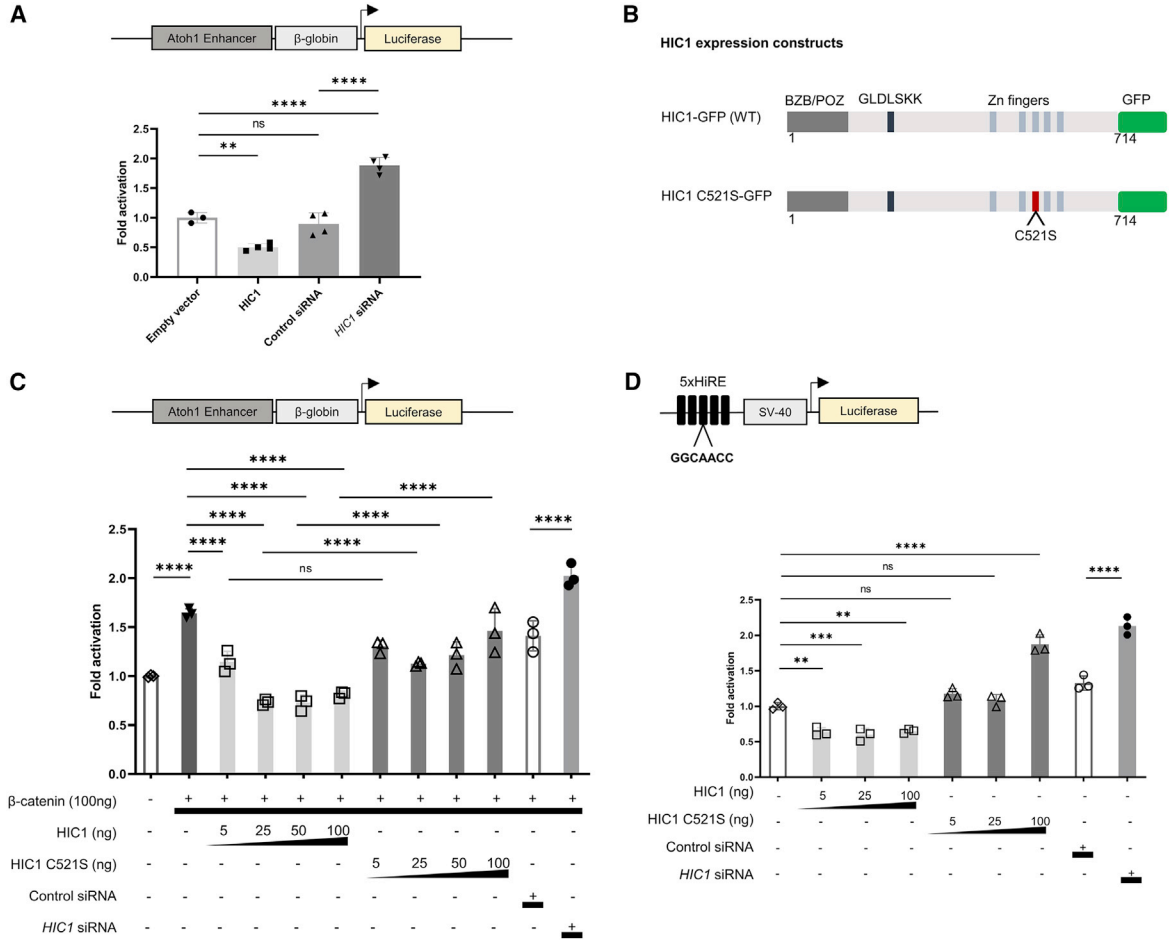

Figure 4. HIC1 Repression is Dependent on DNA Binding

Results of dual luciferase reporter assays in heterologous HEK293 cells are shown.

(A) *Atoh1* enhancer reporter assay in the presence of *HIC1* constitutive overexpression and *HIC1* siRNA-mediated knockdown compared with empty vector and siRNA controls. Consistent with cochlear organoids, *HIC1* overexpression represses, while *HIC1* silencing activates, the *Atoh1* enhancer reporter in HEK293 (n = 4).

(B) Schematic of HIC1 wild-type and C521S expression constructs.

(C) *Atoh1* enhancer reporter assay in the absence (−) or presence (+) of β-catenin, HIC1, HIC1 C521S, and *HIC1* siRNA. HIC1 overexpression mediates dose-dependent suppression of the activating effect of β-catenin on the *Atoh1* enhancer (n = 3). HIC1 C521S is less effective at inhibiting β-catenin-mediated activation of the *Atoh1* enhancer. *HIC1* siRNA potentiates β-catenin activation of the reporter.

(D) HIC1 5×HiRE-luciferase (Pinte et al., 2004) reporter, comprising five minimal HIC1 binding motifs upstream of firefly luciferase, in the presence of HIC1, HIC1 C521S, *HIC1* siRNA, and controls (n = 3). Ectopic expression of HIC1 repressed the reporter. Conversely, HIC1 C521S failed to induce repression of the reporter and lead to de-repression at a higher level. SiRNA targeted to *HIC1* results in relative activation. Reporters, expression constructs, and siRNA were transiently transfected, and firefly luciferase reporter activity was quantified by luminometry, normalized to *Renilla* luciferase signal, and presented as a fold change relative to empty vector control. All experiments were performed on a minimum of three individual occasions, with the n specified. Data reflect mean ± SD; one-way ANOVA, **p < 0.01, ***p < 0.001, ****p < 0.0001.

we studied the interaction between HIC1 and β-catenin on the Wnt reporter. Consistent with the observations of Valenta et al., we found that HIC1 can abolish β-catenin activation of the TCF reporter in a dose-dependent fashion (Figure 5A). HIC1 is not expected to bind the TCF reporter (Valenta et al., 2006), which implies that HIC1 inhibits Wnt and therefore represses *Atoh1* independent of DNA binding. The previously proposed mechanism for this inhibition of Wnt is the formation of HIC1 nuclear bodies that sequester TCF and β-catenin (Valenta et al., 2006), which we observe as well, at least upon HIC1 overexpression (Figure 5B).

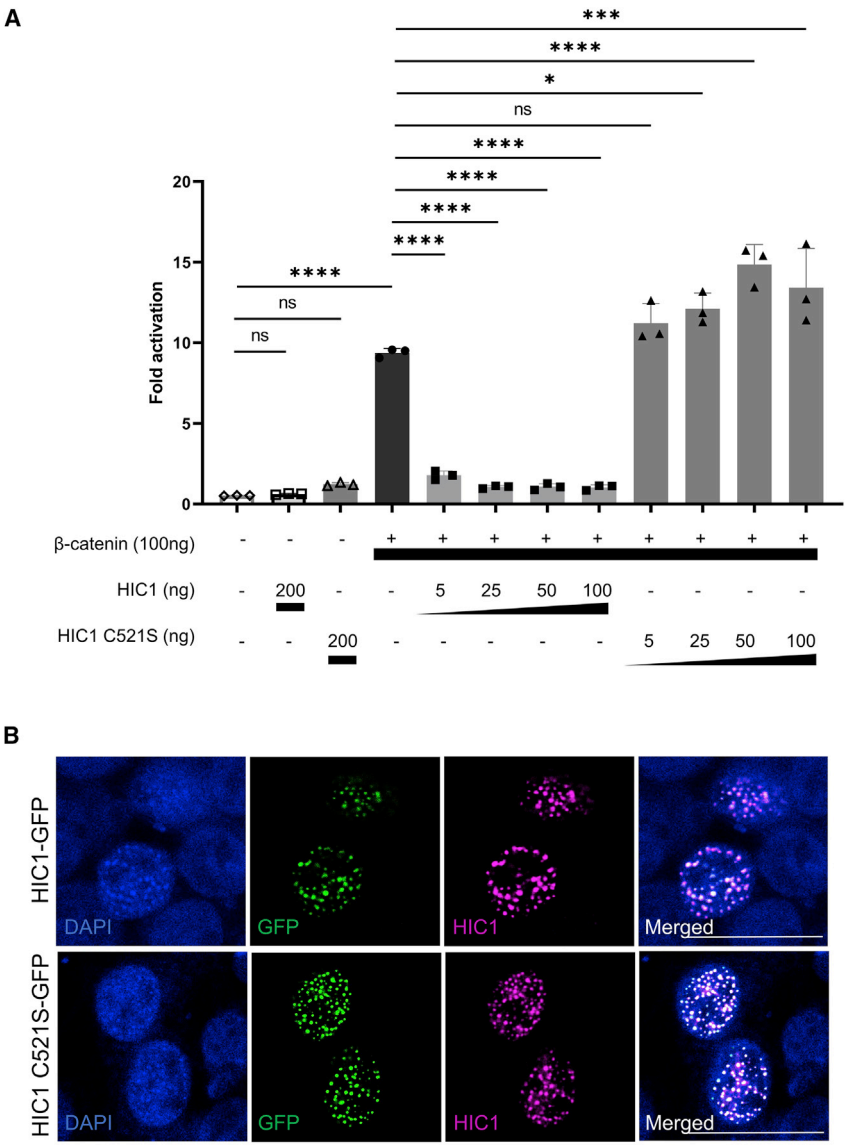

Figure 5. HIC1, but not HIC1 C521S, Represses β-Catenin Activation of TCF Reporter

Results of dual luciferase reporter assays in heterologous HEK293 cells are shown.

(A) TCF reporter pTOPflash assay in the absence (−) or presence (+) of β-catenin, HIC1, and HIC1 C521S at increasing doses. β-catenin potently activates the TCF reporter, which is suppressed by HIC1 in a dose-dependent manner. HIC1 C521S DNA-binding mutant fails to repress β-catenin activation and leads to relative de-repression. Data reflect mean ± SD of normalized firefly/*Renilla* luciferase ratio relative to empty vector control (n = 3 independent experiments); one-way ANOVA, *p < 0.05, ***p < 0.001, ****p < 0.0001.

(B) Representative confocal images of HEK293 cells transfected with HIC1-eGFP (C-terminal tag) and HIC1 C521S-eGFP and stained with anti-HIC1 antibody and DAPI nuclear stain demonstrate that HIC1 and HIC1 C521S are expressed and form "nuclear bodies." Scale bar, 20 μm.

We found no inhibition of pTOPflash reporter activity by the HIC1 mutant C521S (Figure 5A), even though this mutant is still able to form the HIC1 nuclear bodies thought to sequester TCF (Figure 5B). These data suggest that HIC1 C521S may be defective not only in DNA binding but also in its interaction with TCF. In either case, our results indicate that HIC1 can block activation of *Atoh1* by β-catenin and that this interaction is disrupted by mutation of its third zinc-finger domain.

DISCUSSION

Our studies using Atoh1 and Wnt reporter systems demonstrate that HIC1 regulates *Atoh1* expression and sensory hair cell differentiation in the inner ear. These findings suggest a more universal role for HIC1 in repressing *Atoh1* and other Wnt target genes. We observed that silencing *Hic1* alone was sufficient to activate the *Atoh1* enhancer and increase *Atoh1* expression during cochlear progenitor-to-hair cell differentiation, and that this effect was additive when combined with Wnt activation, which potentiates differentiation by upregulating β-catenin. Conversely, HIC1 overexpression significantly inhibited differentiation of progenitor supporting cells to hair cells.

Our findings suggest that HIC1's inhibition of TCF/B-catenin may also rely on zinc-finger-mediated DNA binding. Intriguingly, although the C-terminal region of HIC1 was found to be essential for TCF interaction, Valenta et al. did not observe direct HIC1 binding to the TCF minimal

binding motif (Valenta et al., 2006). The discrepancy between our findings and previous reports may relate to protein characteristics of the mutant in cells versus *in vitro* pull-down assays. We cannot exclude the possibility that the C521S mutation induced a significant structural change that affected the protein beyond DNA binding, though we confirmed that the mutant could be overexpressed and form protein aggregates much akin to wild-type HIC1 without resulting in untoward toxicity. Further work will focus on elucidating the mechanism of this HIC1 C-terminal region in mediating repression of TCF targets.

In the cerebellum, *Hic1* expression is inversely correlated with *Atoh1* expression (Briggs et al., 2008). A correlation between the timing of *Hic1* upregulation and *Atoh1* downregulation in the first few postnatal days supported a similar role for HIC1 in repression of *Atoh1* in the cochlea. *Hic1* expression comes up later and *Atoh1* expression persists longer in the cerebellum (Briggs et al., 2008), and differences in the downstream targets of ATOH1 may explain contrasting roles in the cerebellum and cochlea (Cai and Groves, 2015; Klisch et al., 2011). We found evidence of expression in both hair cells and supporting cells in the postnatal cochlea, which raises the possibility that HIC1 may be contributing to the suppression of *Atoh1* in supporting cells as well as in the maturing hair cells, where *Atoh1* expression precipitously drops, as occurs in CGPs during maturation (Briggs et al., 2008). Recent work that takes advantage of the RiboTag system to enrich for cell-specific expression shows relative enrichment of *Hic1* at least in outer hair cells (using PrestinCreERT2/+; RiboTagHA/+ mice) at various postnatal developmental stages (dataset source: umgear.org) (Hertzano et al., 2020; Matern et al., 2020). Future work will focus on characterizing the significance of changes in *Hic1* expression in the cochlea.

We demonstrate here through shRNA-mediated knockdown of *Hic1* that the expression level is physiologically relevant in suppressing *Atoh1* and hair cell differentiation. Our data on the HIC1 C521S zinc-finger mutant suggest that the repressive effect on the Atoh1 and Wnt reporters more generally is dependent on DNA binding, possibly through recruitment of corepressor complexes. Indeed, HIC1 is known to recruit CtBP, NuRD, and PRC2 in different cellular contexts (Boulay et al., 2012; Deltour et al., 2002; Van Rechem et al., 2010). In turn, HIC1 itself is regulated by HDAC-dependent and independent mechanisms (Deltour et al., 2002), raising the possibility that HDAC inhibitors may be good candidates for (at least in part) reversing HIC1-mediated silencing of *Atoh1* (Dehennaut et al., 2013; Van Rechem et al., 2010). Within the first postnatal week, we and others have shown that, while Wnt signaling is able to induce hair cell differentiation in the newborn, Wnt/β-catenin is no longer effective by as early as P5, despite still being active (Samarajeewa et al., 2018). These observations are consistent with the current pedagogy regarding cellular reprogramming: they imply that transcriptional reprogramming of precursor cells toward a hair cell lineage ultimately requires both forced activation of essential hair cell transcriptional programs and removal of key inhibitory signatures (Hochedlinger and Jaenisch, 2015; Takahashi, 2014; Takahashi et al., 2007). Targeting HIC1, either directly using genetic means (shRNA, CRISPR-Cas9) or indirectly by targeting components of the repressor complexes (e.g., HDAC inhibitors), may potentiate the transcriptional response to Wnt signaling and help drive hair cell differentiation during this period.

Future work will seek to characterize the cochlear-specific HIC1 targets at the *Atoh1* locus and genome-wide and to define the epigenetic changes resulting from *Hic1* knockdown and overexpression and their effects on hair cell differentiation. Additional work will focus on targeting HIC1 *in vivo* to test its role in regeneration in the adult cochlea following hair cell damage. This study supports a growing paradigm wherein repressor complexes recruit epigenetic modifiers that alter key signaling pathways (e.g., Wnt) on fate-determining target genes, like *Atoh1*. Moreover, the use of inner ear organoids to model progenitor-to-hair cell differentiation and targeted knockdown and overexpression, as demonstrated here with HIC1, provides a framework in which to test the effects of candidate factors on hair cell differentiation in a physiologically relevant model. Indeed, elucidating the full repertoire of repressors at the *Atoh1* gene in the inner ear will help instruct efforts in targeted therapy aimed at relieving this repression and potentiating hair cell regeneration.

EXPERIMENTAL PROCEDURES

Experimental Mice

Mice were under the husbandry care of the Massachusetts Eye and Ear Animal Facility. P3 *Atoh1-nGFP* mice (Lumpkin et al., 2003) (provided by Dr. Jane Johnson) were used for organoid dissection to identify differentiated hair cells. Alternatively, for immunohistochemistry/*in situ* hybridization experiments, wild-type C57B6 mice were used at the stated ages. All mouse work was reviewed and approved by the Massachusetts Eye and Ear Animal Care Committee.

Progenitor Cell Isolation and 3D Organoid Culture

Progenitor cells were dissected from the cochlear sensory epithelium and allowed to expand as inner ear organoids using the previously established protocol, with some modifications (Lenz et al., 2019; McLean et al., 2017). Briefly, the sensory epithelium was mechanically dissected from the cochlea with the aid of a cell recovery solution (Corning) and ACCUMAX, and dissociated single cells were embedded in Matrigel (Corning) at a ratio of 1 cochlea per well, in a 24 well plate. Cells were expanded for 10 days in

proliferation medium consisting of valproic acid (1 mM), CHIR (3 μM), 2-phospho-L-ascorbic acid (280 μM), fibroblast growth factor, epidermal growth factor, and insulin growth factor (50 ng/mL each). Organoid proliferation conditions were withdrawn and cells were allowed to differentiate under different treatment conditions. Medium was changed every 2 days.

Plasmid Construction, Lentivirus Production, and Infection

Details of vectors, cloning strategies, and lentivirus production are given in the supplemental information.

In Situ Hybridization Followed by Immunohistochemistry

Single-molecule *in situ* hybridization was performed using the RNAscope 2.0 HD detection kit (Advanced Cell Diagnostics), with a commercially available mRNA probe to *mHic1*, according to the standard fixed protocol, until the final step, when immunostaining was performed prior to mounting (see supplemental experimental procedures).

Immunohistochemistry

Murine cochleae, organoids, and HEK cells were fixed, permeabilized, and blocked, followed by staining using established protocols. Details, including reagents, are provided in the supplemental information.

Organoid Live Cell Imaging

Live organoids were imaged on the Axio Observer Z1 imaging system (Carl Zeiss) and analyzed using Zen 2 software (Carl Zeiss). Laser intensity was kept constant and adjustments for brightness and contrast were kept uniform to allow comparisons of organoids across treatments.

Flow Cytometry

Organoids were dissociated by incubation first in cell recovery solution (Corning), followed by ACCUMAX cell detachment solution. Transduced mScarlet$^+$ cells were isolated on a BD FACS Aria II SORP cell sorter into base medium or RLT buffer (QIAGEN). Dead cells were excluded from the analysis using DAPI staining. FACS plots were analyzed and generated using FlowJo software version 10.4 (Becton Dickinson).

Hair Cell Quantification

Fluorescence images of fixed cochlear organoids at 20× magnification were obtained with an SP8 confocal microscope and formatted with Fiji ImageJ (https://fiji.sc/). MYO7A$^+$ cells were quantified using the Cell Counter plugin from cross-sectional images of mScarlet$^+$ organoids in 5,000 μm^2 regions to account for the variability in organoid size and shape (only regions in the grid that fell completely within an organoid were analyzed, allowing sampling of approximately 80% of a given organoid). Counts were summed across regions and averaged for each organoid. At least 18 mScarlet$^+$ organoids per condition were counted. Statistical analyses were conducted using GraphPad Prism 8.4 software (GraphPad). Two-tailed, unpaired Student's t test was used to determine statistical significance. Data are shown as mean ± SD.

RNA Extraction and qRT-PCR

Fixed cochleae, whole organoids from a single well, and sorted cells were lysed into RLT buffer and total RNA was isolated using the RNeasy Micro Kit (QIAGEN) according to the manufacturer's instructions. RNA was converted to cDNA with the qScript XLT cDNA kit (Quanta BioSciences). qRT-PCR was performed with diluted cDNA (1:4) in two wells for each primer and TaqMan probes and SYBR green master mix (Bio-Rad) on the Bio-Rad iCycler RT-PCR detection system.

Luciferase Assays

HEK293 cells were seeded into 24-well plates one day before transfection. Two hundred fifty nanograms of Atoh1 enhancer-luciferase reporter construct (Shi et al., 2010), or 250 ng of pTOPflash (Molenaar et al., 1996; Shi et al., 2010), with 50 ng of *Renilla* luciferase construct and varying amounts of empty vector (eGFP), HIC1-GFP, HIC1 C521S-GFP, and β-catenin (Shi et al., 2010) expression constructs were transfected using Lipofectamine 2000 per the standard protocol. The total amount of DNA was kept constant. For siRNA experiments, negative control DsiRNA and *HIC1* DsiRNA (hs.Ri.HIC1.13.1) were used at 50 nM final concentration (Integrated DNA Technologies). Cells were lysed after 36 h, and firefly/*Renilla* luciferase activity was measured using the Dual-Glo luciferase reporter assay system (Promega) in a TD-20/20 Luminometer (Turner Designs). Firefly luciferase signal was normalized to *Renilla* luciferase signal and calculated as fold change relative to control.

For the *Atoh1* enhancer-promoter-nanoLuc reporter in inner ear organoids, dissociated cochlear cells were transduced with reporter constructs as well as Tet-pLKOmScarlet-Hic1 according to the above protocol and allowed to expand in Matrigel in a 24 well plate. At the time of differentiation, individual wells were treated with different conditions, with and without 1 μg/mL Dox. Following 10 days of differentiation conditions, the wells were washed with PBS for 1 h and lysed, and nanoLuc/firefly luciferase activity was measured using the Nano-Glo Dual-Luciferase kit (Promega).

Statistical Analysis of Data

The samples used for each experiment are detailed in the figure legends. All experiments were repeated on at least three separate occasions (independent experiments). For organoid assays, one to three wells per group were pooled and analyzed. All center values shown in graphs refer to the mean ± SD. For statistical significance of the differences between the means of two groups, we used two-tailed Student's t tests. Statistical significance for the means of several groups was calculated by performing one-way ANOVA with Tukey's multiple comparisons of the means for each group. A $p < 0.05$ was considered significant. Animals were randomly assigned to groups and contained a mix of male and female littermates.

Data and Code Availability

Source data for HIC1 ChIP-Seq in HEK293 (Figure S3) are available through the ENCODE Project (dataset: ENCSR803GYT, www.encodeproject.org).

SUPPLEMENTAL INFORMATION

Supplemental information can be found online at https://doi.org/10.1016/j.stemcr.2021.02.022.

AUTHOR CONTRIBUTIONS

D.A. and A.E. developed the concepts, analyzed the data, and wrote the manuscript; D.A. designed, performed, and analyzed the experiments; N.H., L.P., and V.S. assisted with experiments and analysis.

ACKNOWLEDGMENTS

We thank Vladamir Korinek for HIC1 plasmids and assistance in the early phase of this project, Dominique LePrince for HIC1 pGL3-5×HiRE-SV40-Luc and other plasmid, and Greg Sienski for the pGS45 overexpression vector. We thank Ronna Hertzano for providing the postnatal OHC RiboTag dataset. We thank the ENCODE Consortium and Michael Snyder for generating the HEK293 HIC1 ChIP-seq dataset. We thank Evgeni Frenkel for critical review and feedback on the manuscript. We thank the Massachusetts General Hospital Pathology and Harvard Stem Cell Institute Cytometry Cores for their expert assistance.

This work was supported by grants from the National Institutes of Health (DC014089), the Capita Foundation, the American Association of Otolaryngology-Head and Neck Surgery (AAO-HNS), and the Hearing Health Foundation.

Received: August 31, 2020
Revised: February 26, 2021
Accepted: February 27, 2021
Published: March 25, 2021

REFERENCES

Abdolazimi, Y., Stojanova, Z., and Segil, N. (2016). Selection of cell fate in the organ of Corti involves the integration of Hes/Hey signaling at the Atoh1 promoter. Development *143*, 841–850.

Atkinson, P.J., Huarcaya Najarro, E., Sayyid, Z.N., and Cheng, A.G. (2015). Sensory hair cell development and regeneration: similarities and differences. Development *142*, 1561–1571.

Ayrault, O., Zhao, H., Zindy, F., Qu, C., Sherr, C.J., and Roussel, M.F. (2010). Atoh1 inhibits neuronal differentiation and collaborates with Gli1 to generate medulloblastoma-initiating cells. Cancer Res. *70*, 5618–5627.

Ben-Arie, N., Hassan, B.A., Bermingham, N.A., Malicki, D.M., Armstrong, D., Matzuk, M., Bellen, H.J., and Zoghbi, H.Y. (2000). Functional conservation of atonal and Math1 in the CNS and PNS. Development *127*, 1039–1048.

Boulay, G., Dubuissez, M., Van Rechem, C., Forget, A., Helin, K., Ayrault, O., and Leprince, D. (2012). Hypermethylated in cancer 1 (HIC1) recruits polycomb repressive complex 2 (PRC2) to a subset of its target genes through interaction with human polycomb-like (hPCL) proteins. J. Biol. Chem. *287*, 10509–10524.

Bramhall, N.F., Shi, F., Arnold, K., Hochedlinger, K., and Edge, A.S. (2014). Lgr5-positive supporting cells generate new hair cells in the postnatal cochlea. Stem Cell Reports *2*, 311–322.

Briggs, K.J., Corcoran-Schwartz, I.M., Zhang, W., Harcke, T., Devereux, W.L., Baylin, S.B., Eberhart, C.G., and Watkins, D.N. (2008). Cooperation between the Hic1 and Ptch1 tumor suppressors in medulloblastoma. Genes Dev. *22*, 770–785.

Brown, R., and Groves, A.K. (2020). Hear, hear for Notch: control of cell fates in the inner ear by Notch signaling. Biomolecules *10*, 370.

Cai, T., and Groves, A.K. (2015). The role of atonal factors in mechanosensory cell specification and function. Mol. Neurobiol. *52*, 1315–1329.

Carter, M.G., Johns, M.A., Zeng, X., Zhou, L., Zink, M.C., Mankowski, J.L., Donovan, D.M., and Baylin, S.B. (2000). Mice deficient in the candidate tumor suppressor gene Hic1 exhibit developmental defects of structures affected in the Miller–Dieker syndrome. Hum. Mol. Genet. *9*, 413–419.

Chai, R., Kuo, B., Wang, T., Liaw, E.J., Xia, A., Jan, T.A., Liu, Z., Taketo, M.M., Oghalai, J.S., Nusse, R., et al. (2012). Wnt signaling induces proliferation of sensory precursors in the postnatal mouse cochlea. Proc. Natl. Acad. Sci. U S A *109*, 8167–8172.

Clevers, H. (2016). Modeling development and disease with organoids. Cell *165*, 1586–1597.

Consortium, E.P. (2012). An integrated encyclopedia of DNA elements in the human genome. Nature *489*, 57–74.

Corwin, J., and Cotanche, D. (1988). Regeneration of sensory hair cells after acoustic trauma. Science *240*, 1772–1774.

Cox, B.C., Chai, R., Lenoir, A., Liu, Z., Zhang, L., Nguyen, D.H., Chalasani, K., Steigelman, K.A., Fang, J., Rubel, E.W., et al. (2014). Spontaneous hair cell regeneration in the neonatal mouse cochlea in vivo. Development *141*, 816–829.

Davis, C.A., Hitz, B.C., Sloan, C.A., Chan, E.T., Davidson, J.M., Gabdank, I., Hilton, J.A., Jain, K., Baymuradov, U.K., Narayanan, A.K., et al. (2018). The Encyclopedia of DNA elements (ENCODE): data portal update. Nucleic Acids Res. *46*, D794–D801.

Dehennaut, V., Loison, I., Dubuissez, M., Nassour, J., Abbadie, C., and Leprince, D. (2013). DNA double-strand breaks lead to activation of hypermethylated in cancer 1 (HIC1) by SUMOylation to regulate DNA repair. J. Biol. Chem. *288*, 10254–10264.

Deltour, S., Pinte, S., Guerardel, C., Wasylyk, B., and Leprince, D. (2002). The human candidate tumor suppressor gene HIC1 recruits CtBP through a degenerate GLDLSKK motif. Mol. Cell Biol. *22*, 4890–4901.

Doetzlhofer, A., White, P., Lee, Y.S., Groves, A., and Segil, N. (2006). Prospective identification and purification of hair cell and supporting cell progenitors from the embryonic cochlea. Brain Res. *1091*, 282–288.

Flora, A., Klisch, T.J., Schuster, G., and Zoghbi, H.Y. (2009). Deletion of Atoh1 disrupts sonic hedgehog signaling in the developing cerebellum and prevents medulloblastoma. Science *326*, 1424–1427.

Gálvez, H., Tena, J.J., Giraldez, F., and Abelló, G. (2017). The repression of Atoh1 by Neurogenin1 during inner ear development. Front. Mol. Neurosci. *10*, 321.

Grausam, K.B., Dooyema, S.D.R., Bihannic, L., Premathilake, H., Morrissy, A.S., Forget, A., Schaefer, A.M., Gundelach, J.H., Macura, S., Maher, D.M., et al. (2017). ATOH1 promotes leptomeningeal

dissemination and metastasis of sonic hedgehog subgroup medulloblastomas. Cancer Res. *77*, 3766–3777.

Grimm, C., Sporle, R., Schmid, T.E., Adler, I.D., Adamski, J., Schughart, K., and Graw, J. (1999). Isolation and embryonic expression of the novel mouse gene Hic1, the homologue of HIC1, a candidate gene for the miller-dieker syndrome. Hum. Mol. Genet. *8*, 697–710.

Helms, A.W., Abney, A.L., Ben-Arie, N., Zoghbi, H.Y., and Johnson, J.E. (2000). Autoregulation and multiple enhancers control Math1 expression in the developing nervous system. Development *127*, 1185–1196.

Hertzano, R., Gwilliam, K., Rose, K., Milon, B., and Matern, M.S. (2020). Cell type–specific expression analysis of the inner ear: a technical report. Laryngoscope.

Hochedlinger, K., and Jaenisch, R. (2015). Induced pluripotency and epigenetic reprogramming. Cold Spring Harb Perspect. Biol. *7*, a019448.

Hu, L., Lu, J., Chiang, H., Wu, H., Edge, A.S., and Shi, F. (2016). Diphtheria toxin-induced cell death triggers wnt-dependent hair cell regeneration in neonatal mice. J. Neurosci. *36*, 9479–9489.

Janeckova, L., Pospichalova, V., Fafilek, B., Vojtechova, M., Tureckova, J., Dobes, J., Dubuissez, M., Leprince, D., Baloghova, N., Horazna, M., et al. (2015). HIC1 tumor suppressor loss potentiates TLR2/NF-kappaB signaling and promotes tissue damage-associated tumorigenesis. Mol. Cancer Res. *13*, 1139–1148.

Jensen, P., Smeyne, R., and Goldowitz, D. (2004). Analysis of cerebellar development in math1 null embryos and chimeras. J. Neurosci. *24*, 2202–2211.

Jeon, S.J., Fujioka, M., Kim, S.C., and Edge, A.S. (2011). Notch signaling alters sensory or neuronal cell fate specification of inner ear stem cells. J. Neurosci. *31*, 8351–8358.

Kelly, M.C., Chang, Q., Pan, A., Lin, X., and Chen, P. (2012). Atoh1 directs the formation of sensory mosaics and induces cell proliferation in the postnatal mammalian cochlea in vivo. J. Neurosci. *32*, 6699–6710.

Klisch, T.J., Xi, Y., Flora, A., Wang, L., Li, W., and Zoghbi, H.Y. (2011). In vivo Atoh1 targetome reveals how a proneural transcription factor regulates cerebellar development. Proc. Natl. Acad. Sci. U S A *108*, 3288–3293.

Lenz, D.R., Gunewardene, N., Abdul-Aziz, D.E., Wang, Q., Gibson, T.M., and Edge, A.S.B. (2019). Applications of lgr5-positive cochlear progenitors (LCPs) to the study of hair cell differentiation. Front. Cell Dev. Biol. *7*, 14.

Lumpkin, E.A., Collisson, T., Parab, P., Omer-Abdalla, A., Haeberle, H., Chen, P., Doetzlhofer, A., White, P., Groves, A., Segil, N., et al. (2003). Math1-driven GFP expression in the developing nervous system of transgenic mice. Gene Expr. Patterns *3*, 389–395.

Matern, M.S., Milon, B., Lipford, E.L., McMurray, M., Ogawa, Y., Tkaczuk, A., Song, Y., Elkon, R., and Hertzano, R. (2020). GFI1 functions to repress neuronal gene expression in the developing inner ear hair cells. Development *147*, dev186015.

McLean, W.J., Yin, X., Lu, L., Lenz, D.R., McLean, D., Langer, R., Karp, J.M., and Edge, A.S.B. (2017). Clonal expansion of lgr5-positive cells from mammalian cochlea and high-purity generation of sensory hair cells. Cell Rep. *18*, 1917–1929.

Mizutari, K., Fujioka, M., Hosoya, M., Bramhall, N., Okano, H.J., Okano, H., and Edge, A.S. (2013). Notch inhibition induces cochlear hair cell regeneration and recovery of hearing after acoustic trauma. Neuron *77*, 58–69.

Molenaar, M., Van De Wetering, M., Oosterwegel, M., Peterson-Maduro, J., Godsave, S., Korinek, V., Roose, J., Destrée, O., and Clevers, H. (1996). XTcf-3 transcription factor mediates β-catenin-induced Axis formation in Xenopus embryos. Cell *86*, 391–399.

Pinte, S., Stankovic-Valentin, N., Deltour, S., Rood, B.R., Guerardel, C., and Leprince, D. (2004). The tumor suppressor gene HIC1 (hypermethylated in cancer 1) is a sequence-specific transcriptional repressor: definition of its consensus binding sequence and analysis of its DNA binding and repressive properties. J. Biol. Chem. *279*, 38313–38324.

Pospichalova, V., Tureckova, J., Fafilek, B., Vojtechova, M., Krausova, M., Lukas, J., Sloncova, E., Takacova, S., Divoky, V., Leprince, D., et al. (2011). Generation of two modified mouse alleles of the Hic1 tumor suppressor gene*49*, 142–151.

Roccio, M., and Edge, A.S.B. (2019). Inner ear organoids: new tools to understand neurosensory cell development, degeneration and regeneration. Development *146*, dev177188.

Ryals, B., and Rubel, E. (1988). Hair cell regeneration after acoustic trauma in adult Coturnix quail. Science *240*, 1774–1776.

Samarajeewa, A., Lenz, D.R., Xie, L., Chiang, H., Kirchner, R., Mulvaney, J.F., Edge, A.S.B., and Dabdoub, A. (2018). Transcriptional response to Wnt activation regulates the regenerative capacity of the mammalian cochlea. Development *145*, dev166579.

Shi, F., Cheng, Y.-F., Wang, X.L., and Edge, A.S.B. (2010). β-Catenin up-regulates Atoh1 expression in neural progenitor cells by interaction with an Atoh1 3′ Enhancer. J. Biol. Chem. *285*, 392–400.

Shi, F., Hu, L., and Edge, A.S. (2013). Generation of hair cells in neonatal mice by beta-catenin overexpression in Lgr5-positive cochlear progenitors. Proc. Natl. Acad. Sci. U S A *110*, 13851–13856.

Takahashi, K. (2014). Cellular reprogramming. Cold Spring Harb Perspect. Biol. *6*, a018606.

Takahashi, K., Tanabe, K., Ohnuki, M., Narita, M., Ichisaka, T., Tomoda, K., and Yamanaka, S. (2007). Induction of pluripotent stem cells from adult human fibroblasts by defined factors. Cell *131*, 861–872.

Valenta, T., Lukas, J., Doubravska, L., Fafilek, B., and Korinek, V. (2006). HIC1 attenuates Wnt signaling by recruitment of TCF-4 and beta-catenin to the nuclear bodies. EMBO J. *25*, 2326–2337.

Van Rechem, C., Boulay, G., Pinte, S., Stankovic-Valentin, N., Guerardel, C., and Leprince, D. (2010). Differential regulation of HIC1 target genes by CtBP and NuRD, via an acetylation/SUMOylation switch, in quiescent versus proliferating cells. Mol. Cell Biol. *30*, 4045–4059.

Warchol, M.E. (2011). Sensory regeneration in the vertebrate inner ear: differences at the levels of cells and species. Hear Res. *273*, 72–79.

White, P.M., Doetzlhofer, A., Lee, Y.S., Groves, A.K., and Segil, N. (2006). Mammalian cochlear supporting cells can divide and trans-differentiate into hair cells. Nature *441*, 984–987.